

Spark Ignition in a Turbulent Shearless Fuel-air Mixing Layer: Average Flame Growth Rates

S.F. Ahmed^{*}, I.A. Bahena Ledezma[†], and E. Mastorakos[‡]

Engineering Department, University of Cambridge, Cambridge, CB2 1PZ, UK

A planar methane-air mixing layer with equal velocity in the two streams and approximately homogeneous turbulent intensity and lengthscale has been used to examine non-premixed edge flame speed following spark ignition. The flame was visualized with a high-speed camera and the flame's edges in the upstream, downstream and cross-stream directions have been identified and their average rate of evolution allowed an estimate of the average absolute flame speed. By subtracting the uniform mean velocity resulted in estimates of the mean relative edge flame speed. This quantity was approximately $2.5S_L$, where S_L is the laminar burning velocity of stoichiometric methane-air premixed flames. The results are consistent with DNS of turbulent edge flames.

Nomenclature

H	=	channel height [m]
M	=	diameter of holes in perforated plate [m]
S_L	=	laminar burning velocity of stoichiometric mixture [m/s]
t	=	time [s]
u'	=	streamwise r.m.s. turbulent velocity fluctuations [m/s]
U	=	streamwise mean velocity [m/s]
U_b	=	bulk velocity [m/s]
W	=	channel width [m]
x	=	streamwise coordinate [m]
y	=	cross-stream coordinate (normal to splitter plate) [m]
z	=	cross-stream coordinate (parallel to splitter plate) [m]

I. Introduction

Spark ignition of non-premixed combustion is important in high-altitude reflight of aviation gas turbines, in industrial furnaces, and in some GDI automotive engines. Our physical understanding of such processes is not yet at a point that quantitative theoretical predictions can be made. Experiments with spark ignition of jet diffusion flames^{1,2} showed that the probability of the emergence of an initial flame kernel in the spark neighbourhood is approximately equal to the probability of finding air-fuel mixture within the flammability limits. This concept has been further explored to provide a quantitative explosion risk assessment³ with CFD and a presumed shape of the PDF of the mixture fraction. Recently, spark ignition of non-premixed flames has been re-visited with jet⁴, counter-flow⁵, and bluff-body methane flames⁶. It was shown that, if ignition means the achievement of a full diffusion flame and not just the emergence of a small kernel that may be convected with the flow without causing flame ignition, the ignition probability is reduced and can be zero even in locations that have finite probability of flammable mixture fractions. The difference was attributed to local strain effects or high velocities that may not allow the flame kernel to grow or a flame to propagate, despite the local mixture fraction being flammable. In addition, the non-local effects, heat convection from the spark for instance, can play a very important part in determining the success of ignition⁵, so that the ignition probability was finite even in regions of zero probability of finding flammable mixtures. Simulations of spark ignition in a laminar non-premixed counterflow flame⁷ reproduced these conjectures: ignition of the stoichiometric fluid could be achieved due to heat diffusion from the sparked region, even if that was

^{*} Post-doctoral researcher, Engineering Department, University of Cambridge, Cambridge, CB2 1PZ, UK.

[†] Visiting Masters student, ENSEEIHT, Toulouse, France.

[‡] Reader, Engineering Department, University of Cambridge, CB2 1PZ, UK. Email: em257@eng.cam.ac.uk

located at rich or lean positions, and there was a critical strain rate, depending on the spark position and energy, above which ignition could not be achieved.

One additional reason why the ignition probability is less than unity, and why it is different than the probability of just establishing a small kernel, is that the flame cannot propagate against the flow to ignite the whole combustor. This, for example, has been visualized in simple recirculating flames⁶, but also in realistic gas turbine combustors⁸. Hence, to understand this problem better, the speed at which flames propagate in turbulent non-premixed reactants must be quantified. This propagation takes place, in principle, along the stoichiometric mixture fraction contour. When the mixture fraction fluctuates little about a nominally flammable value, so that it is always lean or always rich, premixed flame concepts can be used to describe flame propagation⁹⁻¹¹. We may call this “stratified-charge premixed flame”. When the mixture fraction fluctuates around the stoichiometric value, combustion occurs in a lean premixed, rich premixed, and non-premixed mode and the flame structure is reminiscent of so-called triple flames, which can merge under high strain rate to become edge flames¹². Propagation of turbulent flames in this mode, which could be called “turbulent non-premixed edge flame”, has not been studied well enough, although some relevant information has become available from studies on turbulent jet lifted flames¹³⁻¹⁴. In particular, from analyzing high-speed images of the flame at the stabilization height in jet flames¹⁴, it has been concluded that the average edge flame speed is of the same order as the laminar burning velocity of the stoichiometric mixture S_L . The relative speed (i.e. flame edge speed relative to the fluid immediately ahead of the triple point) has been measured in the counterflow configuration¹⁵ and its average value was around $0.75 S_L$. Similar data from Direct Numerical Simulations of spark ignition and ensuing flame propagation in turbulent mixing layers in isotropic decaying turbulence¹⁶⁻¹⁸ have revealed the detrimental effects of intense turbulence on absolute and relative edge flame propagation speed¹⁶⁻¹⁷ and the effects of mixture fraction gradient and spark position on the structure and speed of the flame¹⁸.

A detailed experiment study of spark ignition and flame propagation in the canonical problem of the turbulent mixing layer has not been performed yet. Hence, in this paper, we present the characteristics of such a fuel-air mixing layer and we examine the propagation speed (relative to fixed coordinates) of the flame edge, as it expands along the layer. This propagation occurs against the flow on one side of the flame, with the flow on the other side, and against zero mean flow in the direction across the mean flow (parallel to the mixing layer). Hence the experiment allows various insights into edge flame propagation. The fact that the flow velocity is uniform facilitates an estimate of the average relative propagation speed. The experimental methods are presented next, while the results are presented and discussed in Section III.

II. Experimental Methods

The burner (Fig.1) consists of two stainless steel channels with rectangular cross-section, whose two sides are $W=46$ mm and 20.5 mm, both being 500 mm long. The walls of the channels have a thickness of 2.5 mm. The two channels are attached along their length and their common wall is machined to produce a slope of 2.5 degrees, which results essentially in a splitter plate separating the two flows. At the edge of this plate (the exit of the channels), the height of each channel is $H/2=23$ mm. A quartz section of width W and height H is then fitted to provide optical access to the planar mixing layer formed downstream of the splitter plate between the flows in the two channels. A perforated plate with 40% solidity and holes of size $M=3$ mm is fitted 50 mm upstream of the splitter plate edge (Fig. 1).

One channel carries air from the laboratory compressor and the other a fuel-air mixture. The fuel was methane (99.96% purity) and was mixed with 80% air (by vol.). At this level of premixedness, the fuel-air stream is above the rich flammability limit and hence the flame formed between the two streams is of non-premixed character. The air and fuel stream velocities at the exit were equal and, for most of the experiments reported here, the bulk velocities were $U_b=3.0$ m/s and, for some experiments, $U_b=1.5$ m/s. Both air and fuel flow rates were controlled by mass flow controllers. The Reynolds number of the flow in the channel before the perforated plate was 6720 (based on the hydraulic diameter).

The experiment has been designed in an effort to reproduce, at a smaller scale and adapted to the limitations imposed by safely performing a lab-scale combustion experiment, the shearless turbulent mixing layer studied experimentally by Ma and Warhaft¹⁹. It is also the experimental analogue of the DNS studied previously¹⁶⁻¹⁸. In particular, this experiment has turbulent Reynolds numbers close to those in the DNS, which facilitates some comparisons.

To measure the streamwise (x) component of the velocity at various locations, a hot wire system was employed. A single constant-temperature Dantec 55P16 platinum-plated tungsten hot wire (diameter 5 μm and length 1.25 mm)

was used with a DISA 55M01 standard bridge. The hot wire was placed perpendicular to the main flow direction and aligned with the z -direction. The measurements were taken with 10 kHz sampling rate and about 60,000 samples were recorded at each location using a DAQ system. The maximum statistical uncertainty for the reported mean velocities is estimated as 2%. All velocities reported are from the unignited condition.

An ignition system was especially designed to produce repeatable sparks whose energy and duration could be varied independently. The main features of the unit can be found in Ref. 4. The spark was created between two tungsten electrodes of 1 mm diameter, which were placed as shown in Fig. 1 to ensure minimum disturbance to the flow field. The electrodes had pointed edges to reduce the heat loss from the spark and the distance between them was 2 mm. The two electrodes were attached to a twin-bore ceramic tube, which was traversed axially and radially to cover the whole flow field with 0.1 mm resolution. For the experiments described here, the spark had duration of 400 μ s and the electrical energy delivered by the circuit was 100 mJ.

The ignition event was monitored with a Phantom V4.2 Digital High Speed Camera fitted with a fast intensifier. A number of movies were captured with 4200 fps for successful and failed ignition events at different locations in the flow field in order to understand the behavior and the structure of the flame front from the moment of the spark until the establishment of the full planar turbulent flame or until blow-out of the domain. The images were imported to Matlab. For each image, a first stage of filtering removed noise, while a threshold was used at a second stage to detect the flame edge. This was done while traversing the domain from the clear area towards the flame zone. Therefore, the upstream, cross-stream and downstream flame edges were detected as a function of time for about 40 ms from the spark in each movie. A total of 40 such movies were made, from which average quantities were calculated.

III. Results and Discussion

A. Flame Visualization

Figure 1 shows photographs of the flame at a relatively low velocity, namely $U_b=1.5$ m/s. At this velocity, the wake behind the splitter plate has low enough velocities to allow flame stabilization and hence, following ignition at a point downstream, the flame always eventually propagated back towards the splitter plate to attach there. It is evident that the flame is planar and that the flame brush thickens downstream, probably due to the mixing layer growth.

Figure 2 shows snapshots during the flame evolution following a spark, with the flow at $U_b=1.5$ m/s, a condition that leads to attached flames. The flame expands quickly in the downstream and the cross-stream directions (e.g. image at $t=35.7$ ms) and slowly propagates upstream against the incoming flow to eventually attach at the splitter plate (see image at $t=178.5$ ms). The flame outline is clearly turbulent and quite sharp, which can lead to a determination of the flame edge. Figure 3 shows similar snapshots during the flame evolution at $U_b=3.0$ m/s, a condition that leads to flame growth but no stabilization. For this condition, the downstream edge of the flame is convected out of the viewing window, as expected. The upstream edge is also being convected downstream, but at a slower rate than the downstream edge. In the cross-stream direction, the flame has filled the channel at a time that is somewhat earlier for the high velocity case than for the lower velocity case.

B. Velocity measurements

Figure 4 shows mean and r.m.s. velocities at various locations. The mean velocity is approximately uniform away from the splitter plate, but a thin wake immediately downstream of the splitter plate is evident. This wake region has low enough velocity (for the $U_b=1.5$ m/s case) that flame propagation upstream and stabilization becomes possible. For the $U_b=3.0$ m/s case, the mean velocity is larger, which prevents stabilization. As we go downstream, the mean velocity becomes uniform in the y - and z -directions.

The r.m.s. velocity is also quite uniform across the channel, even across the wake. At $x=3$ mm, u' is about 0.5 m/s (about 15% of the bulk velocity), decaying to about 0.25 m/s by $x=83$ mm. From measurements of the autocorrelation and using the Taylor hypothesis, the turbulent lengthscale was found to be approximately 7 mm at $x=3$ mm, growing to about 8 mm by $x=83$ mm.

Detailed measurements of the mixture fraction (done by acetone PLIF) will be presented in the full paper to facilitate interpretation of the flame speed data.

C. Edge flame velocity

Figure 5 shows schematically a typical flame outline following spark ignition at a point when the flow is at a velocity that does not permit upstream propagation and stabilisation. The flame grows, as it is being convected

downstream. The most upstream edge of the flame is denoted by X_u , the most downstream edge is denoted as X_d , the left-most edge by Z_l , and the right-most edge by Z_r . These quantities are extracted from each image from a sequence captured by the high speed camera.

Figure 6 shows examples of the time evolution of the flame edge location from ten separate ignition events. The average position, calculated over 40 movies, is superimposed. It is evident that there is a shot-to-shot variation and that, during the evolution of the edge, its speed (understood as the slope of the curve with respect to time) is not constant. The downstream edge moves out of the domain after about 10 ms, while the upstream edge takes about 25 ms to be convected out of the imaged region. In the homogeneous (z) direction, after about 2 ms the flame begins to expand at a relatively constant rate. The initial quick expansion due to the spark is evident by the fact that at about 0.5 ms from the initiation of the spark ($t=0$), the flame kernel has a diameter of about 4-5 mm.

Figure 7 shows the mean velocities of the flame after subtracting the mean velocity of the flow in the corresponding direction. This gives an estimate of the mean flame edge relative velocity. It is evident that: (i) differentiating the mean flame position results in a very noisy trace, especially for the streamwise direction; (ii) from between 4 to 10 ms, the relative speed is fluctuating less; and finally (iii) the two cross-stream directions give similar absolute speeds, as expected.

To avoid the uncertainties associated with differentiating experimental data, linear fits have been performed to the mean edge flame positions (Fig. 8). So, an estimate of the downstream edge flame absolute speed ($d\langle X_d \rangle / dt$) is 4.53 m/s, giving an estimate of the downstream relative speed ($d\langle X_d \rangle / dt - U_b$) of 1.53 m/s; for the upstream edge, the mean absolute speed is $d\langle X_u \rangle / dt = 2.1$ m/s, giving a mean relative speed of $U_b - d\langle X_u \rangle / dt = 0.9$ m/s; while the two cross-stream velocities ($d\langle Z_l \rangle / dt$ and $d\langle Z_r \rangle / dt$) are very close (0.99 and 1.0 m/s). There is no mean flow in the cross-stream direction, hence the absolute velocities that have been measured can serve as estimates of the relative velocity.

It is clear that the mean relative edge flame speeds in the three directions (upstream and the two cross-stream) are approximately equal. For laminar edge flames, the estimate $(\rho_u / \rho_b)^{1/2} S_L$, where S_L is the laminar burning velocity of the stoichiometric mixture, ρ_u the unburnt gas density and ρ_b the burnt-gas density, provides a good estimate of the absolute edge flame propagation speed in stagnant fluid¹². For methane, $S_L = 0.4$ m/s and $\rho_u / \rho_b = 7.4$ (for ambient conditions of reactants), which results in an edge flame speed of 1.1 m/s. Hence, for the present turbulent edge flame, the mean propagation speed is close to the result from laminar edge flames. This is fully consistent with DNS data¹⁶, which provides credence to the present experimental measurements.

In the downstream direction, the estimated relative speed is higher than this. This may be due to the expansion of the flow in the burnt region, which is expected to accelerate the mean flow in the streamwise direction. Note that the present estimates of flame speed are based on the mean flow velocity far from the flame edge, i.e. without taking the local flow expansion into account. When this expansion is taken into account, the flame edge relative to the flow velocity immediately ahead of the flame edge may be smaller than S_L , as found from experiments¹⁵ and DNS¹⁷.

Further understanding on the edge flame absolute velocity can be provided by similar measurements at different bulk velocities, which will be presented in the full paper. In addition, further estimates to include heat release effects will be made. The data can help with the design of practical ignition systems in realistic combustors and the development of advanced combustion models.

IV. Conclusions

A planar methane-air mixing layer with equal velocity in the two streams and approximately homogeneous turbulent intensity and lengthscale has been developed and has been used to examine flame speed following spark ignition. The flame was visualized with a high-speed camera and the flame's edges in the upstream, downstream and cross-stream directions have been identified. Their average rate of evolution allowed an estimate of the average absolute flame speed, while by subtracting the uniform mean velocity, estimates of the mean relative edge flame speed were made. The results show that this quantity was approximately 1 m/s, which corresponds to about $2.5 S_L$. The results are consistent with DNS of turbulent non-premixed edge flames.

Acknowledgments

This work has been funded by the European Commission through project "TIMECOP-AE" (AST5-CT-2006-030828).

References

1. A. D. Birch, D. R. Brown, and M. G. Dodson. Ignition probabilities in turbulent mixing flows. *Proceedings of the Combustion Institute*, 18:1775-1780, 1981.
2. M. T. E. Smith, A. D. Birch, D. R. Brown, and M. Fairweather. Studies of ignition and flame propagation in turbulent jets of natural gas, propane and a gas with a high hydrogen content. *Proceedings of the Combustion Institute*, 21:1403-1408, 1986.
3. R. F. Alvani and M. Fairweather. Ignition characteristics of turbulent jet flows. *Chemical Engineering Research and Design*, 80:917-923, 2002.
4. S. F. Ahmed and E. Mastorakos. Spark ignition of lifted turbulent jet flames. *Combustion and Flame*, 146:215-231, 2006.
5. S. F. Ahmed, R. Balachandran, and E. Mastorakos. Measurements of ignition probability in turbulent non-premixed counterflow flames. *Proceedings of the Combustion Institute*, 31:1507-1513, 2007.
6. S. F. Ahmed, R. Balachandran, T. Marchione, and E. Mastorakos. Spark ignition of turbulent non-premixed bluff-body flames. *Combustion and Flame*, 151:366-385, 2007.
7. E. S. Richardson and E. Mastorakos. Numerical investigation of forced ignition in laminar counterflow non-premixed methane-air flames. *Combustion Science and Technology*, 179:21-37, 2007.
8. R. W. Read, J. W. Rogerson, and S. Hochgreb. Relight imaging at low temperature, low pressure conditions. *AIAA Paper*, pages AIAA-2008-0957, 2008.
9. T. Kang and D. C. Kyritsis. Methane flame propagation in compositionally stratified gases. *Combustion Science and Technology*, 177:2191-2210, 2005.
10. R. W. Bilger, S. B. Pope, K. N. C. Bray, and J. F. Driscoll. Paradigms in turbulent combustion research. *Proceedings of the Combustion Institute*, 30:21-42, 2005.
11. N. Pasquier, B. Lecordier, M. Trinite, and A. Cessou. An experimental investigation of flame propagation through a turbulent stratified mixture. *Proceedings of the Combustion Institute*, 31:1567-1574, 2007.
12. J. Buckmaster. Edge-flames and their stability. *Combustion Science and Technology*, 115:41-68, 1996.
13. K. M. Lyons. Toward an understanding of the stabilization mechanisms of lifted turbulent jet flames: Experiments. *Progress in Energy and Combustion Science*, 33:211-231, 2007.
14. A. Upatnieks, J.F. Driscoll, C.C. Rasmussen, S.L. Ceccio. Title. *Combustion and Flame*, 138:259-272, 2004.
15. C. Heeger, B. Böhm, S.F. Ahmed, R. Gordon, I. Boxx, W. Meier, A. Dreizler, E. Mastorakos. Statistics of Relative and Absolute Velocities of Turbulent Non-premixed Edge Flames Following Spark Ignition. To be presented at the 32nd International Symposium on Combustion, Montreal, August 2008.
16. N. Chakraborty, E. Mastorakos, and R. S. Cant. Effects of turbulence on spark ignition in inhomogeneous mixtures: a direct numerical simulation (DNS) study. *Combustion Science and Technology*, 179:293-317, 2007.
17. N. Chakraborty and E. Mastorakos. Numerical investigation of edge flame propagation characteristics in turbulent mixing layers. *Physics of Fluids*, 18:105103, 2006.
18. N. Chakraborty and E. Mastorakos. Direct numerical simulations of localised forced ignition in turbulent mixing layers: the effects of mixture fraction and its gradient. *Flow, Turbulence and Combustion*, 80:155-186, 2008.
19. B.K. Ma and Z. Warhaft. Some aspects of the thermal mixing layer in grid turbulence. *Physics of Fluids*, 29: 3114 -3120, 1986.

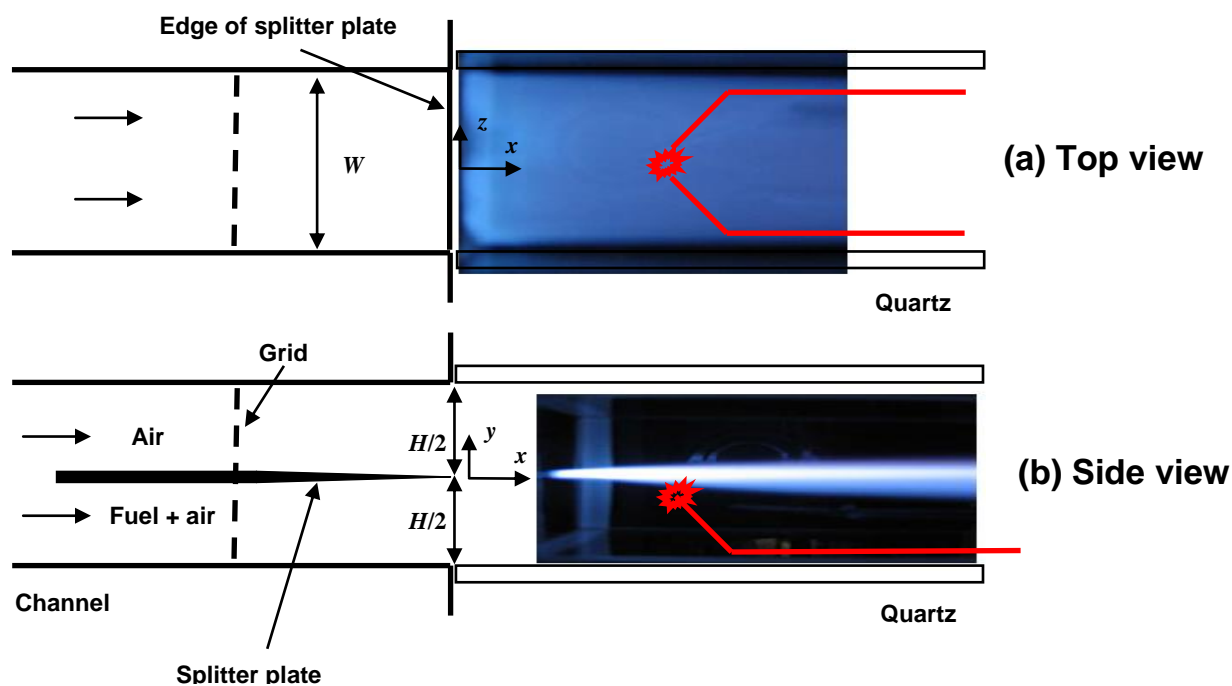


Figure 1. Schematic diagram of the test rig and photographs of the attached flame at $U_b=1.5\text{m/s}$. In the side view (b), the photo has been shifted to the right for clarity. The spark location and electrodes orientation is also shown by the thick red lines.

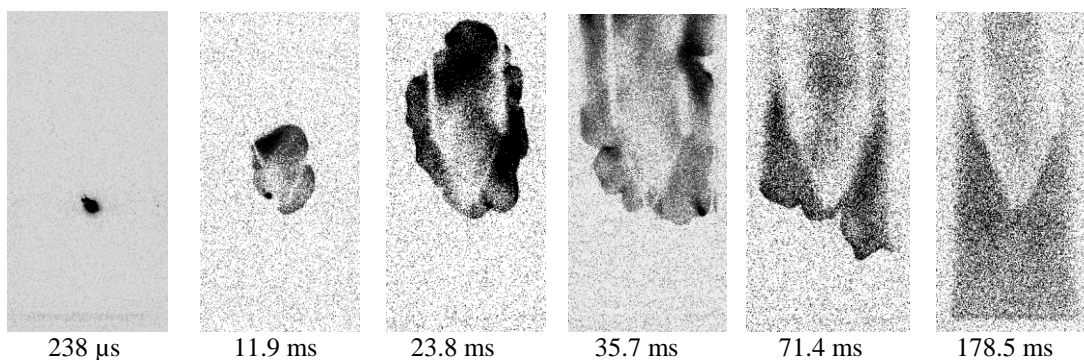


Figure 2. Snapshots of flame following ignition at $U_b=1.5\text{m/s}$. Top view (through the air stream), the flow comes from below. Camera settings: 4200 frames per second, exposure time: $228\ \mu\text{s}$. Image domain is $100\times 52\ \text{mm}$. The electrodes are visible due to the light emission from the flame. Spark at $x=40\text{mm}$, $y=z=0$.

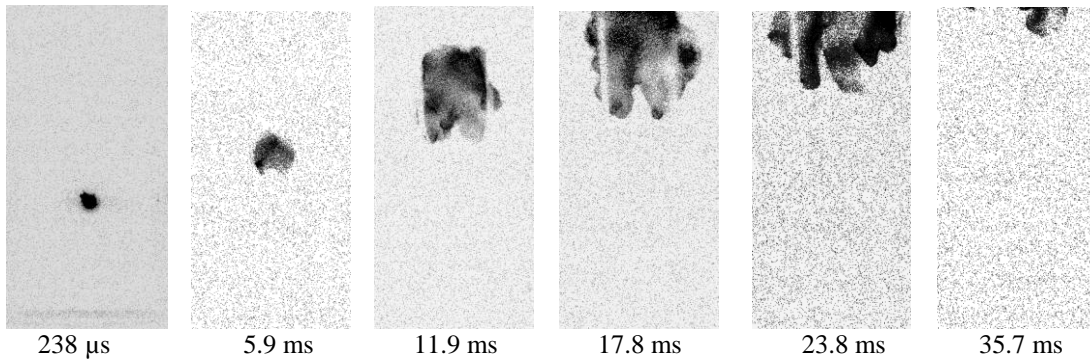


Figure 3. Snapshots of flame following ignition at $U_b=3.0\text{m/s}$. All other parameters are as in Fig. 2.

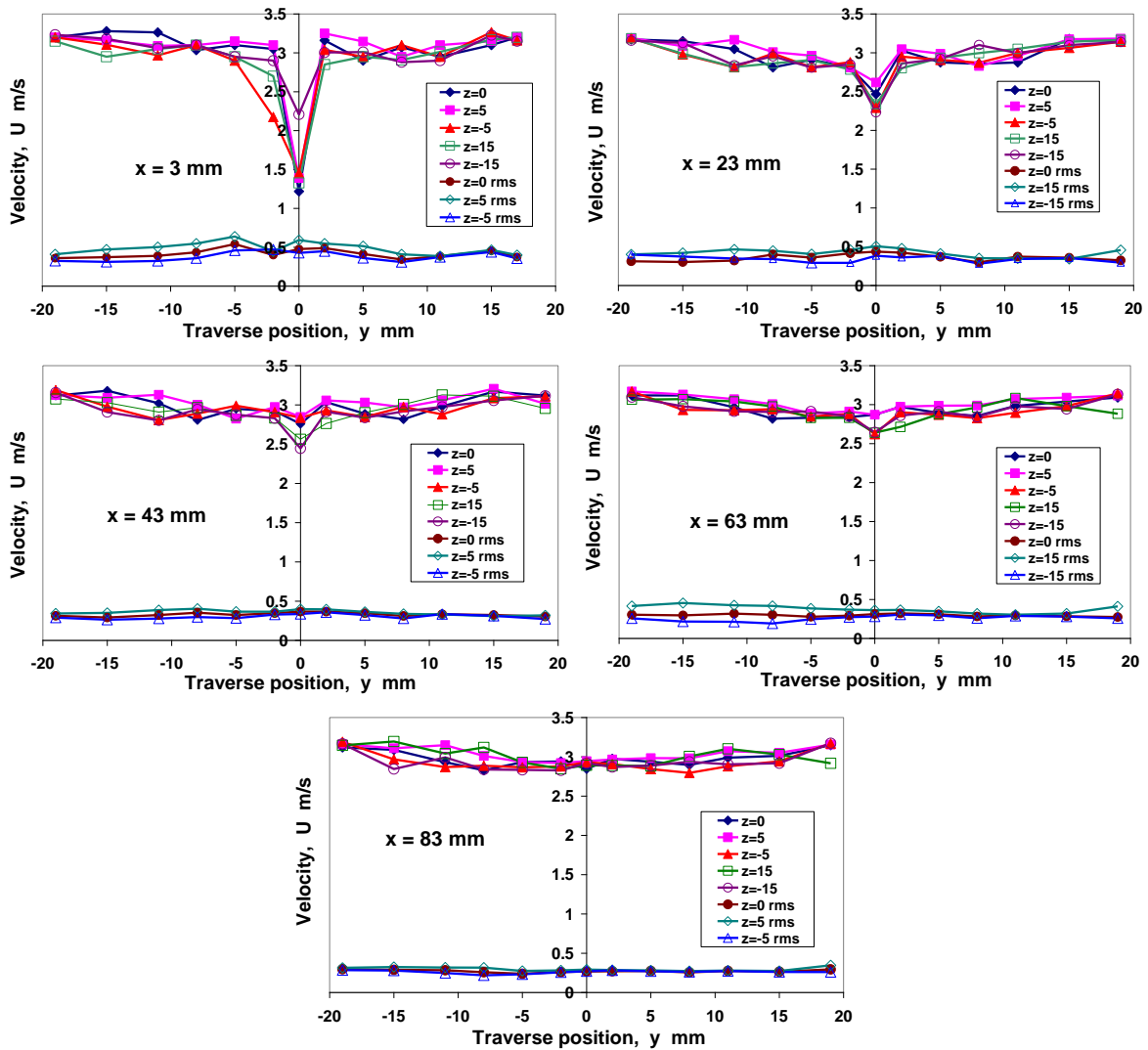


Figure 4. Mean and r.m.s. streamwise velocities at the indicated distance from the splitter plate edge. Flow condition: $U_b=3.0\text{m/s}$.

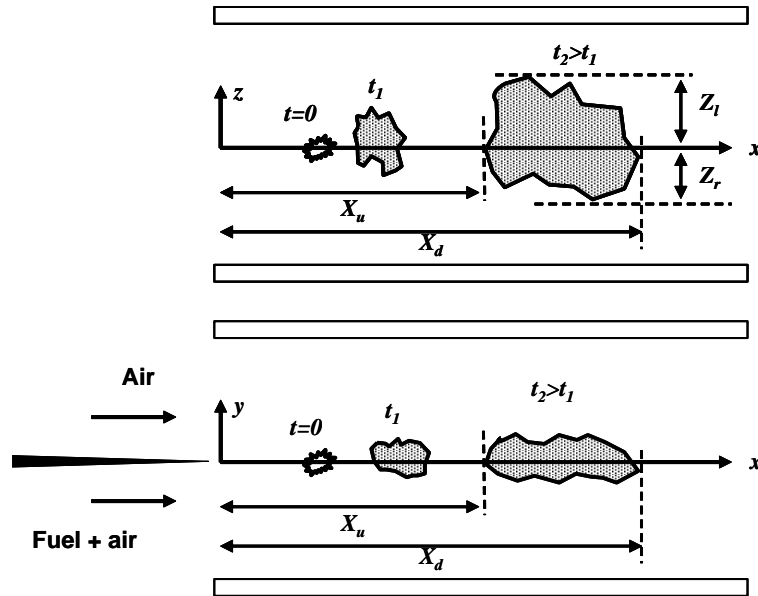


Figure 5. Sketch defining the edges of the flame from a top view of the expanding flame (as in Figs. 1a, 2 and 3) (upper sketch) and a side view (lower sketch). The flow comes from the left. The quantities X_u , X_d , Z_l , and Z_r are found as a function of time from each movie.

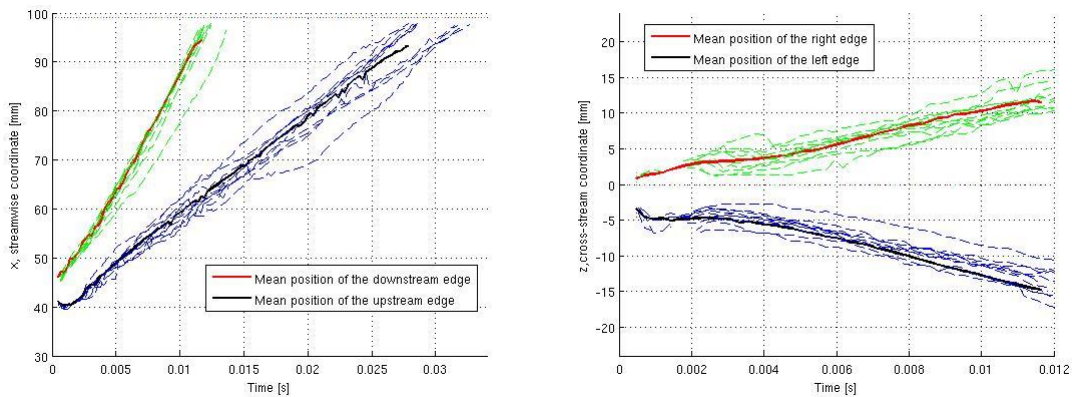


Figure 6. A few time evolutions of X_u and X_d (left) and Z_l and Z_r (right) from individual movies and the corresponding averages compiled over 50 movies denoted by thick lines. Flow conditions: $U_b=3.0\text{m/s}$ and sparking at $x=40\text{mm}$, $y=0$, $z=0$.

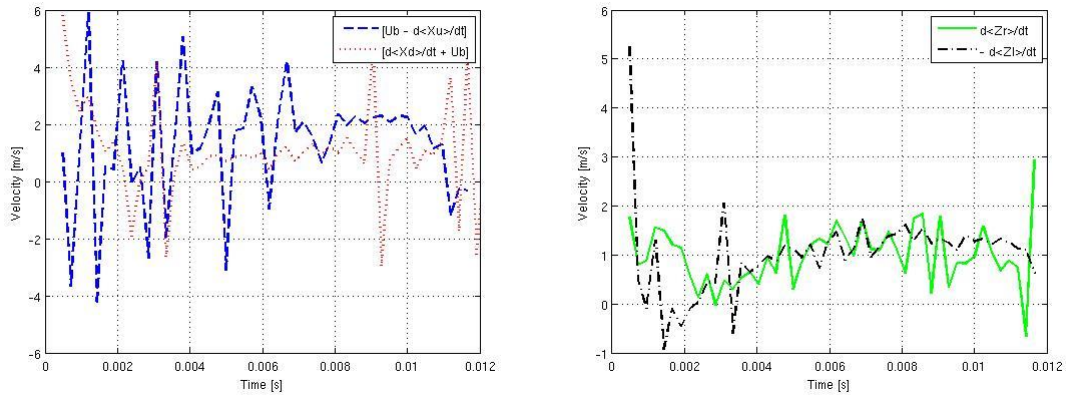


Figure 7. The time evolutions of $[U_b - d\langle X_u \rangle / dt]$ and $[d\langle X_d \rangle / dt - U_b]$ (left), and $d\langle Z_r \rangle / dt$ and $-d\langle Z_l \rangle / dt$ (right). Flow conditions: $U_b=3.0\text{m/s}$ and sparking at $x=40\text{mm}$, $y=0$, $z=0$.

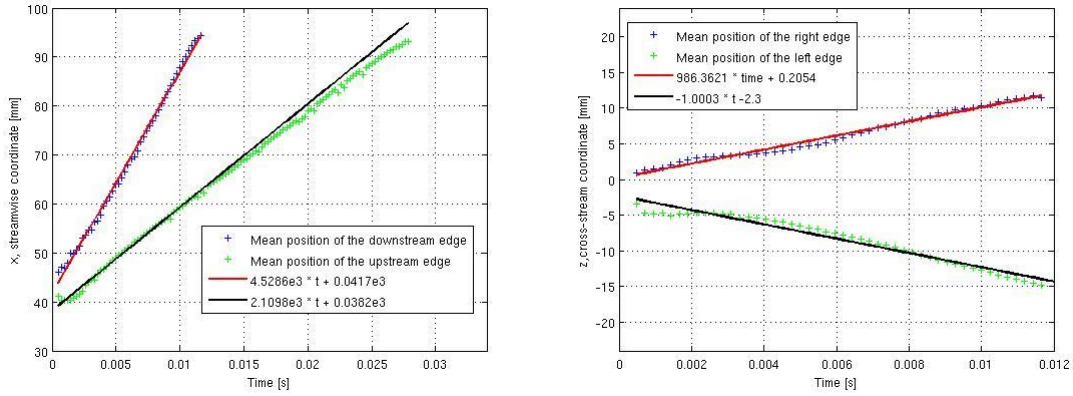


Figure 8. Linear curve fits to the mean flame edge position data of Fig. 6.